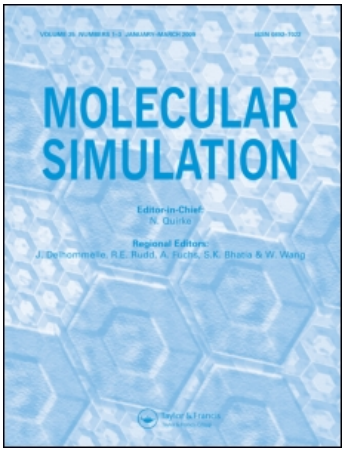

Molecular Simulation
Publication details, including instructions for authors and subscription information:
http://www.informaworld.com/smpp/title~content=t713644482

A Molecular Dynamics Investigation of Chain Conformational Changes In Compressed Bilayers

J. Corish[a]; D. A. Morton-blake[a]
[a] Chemistry Dept., Trinity College, Dublin, Ireland

To cite this Article Corish, J. and Morton-blake, D. A.(2000) 'A Molecular Dynamics Investigation of Chain Conformational Changes In Compressed Bilayers', Molecular Simulation, 25: 6, 339 — 360
To link to this Article: DOI: 10.1080/08927020008028166
URL: http://dx.doi.org/10.1080/08927020008028166

Molecular Simulation, 2000, Vol. 25, pp. 339–360
Reprints available directly from the publisher
Photocopying permitted by license only

A MOLECULAR DYNAMICS INVESTIGATION OF CHAIN CONFORMATIONAL CHANGES IN COMPRESSED BILAYERS

J. CORISH and D. A. MORTON-BLAKE*

Chemistry Dept., Trinity College, Dublin 2, Ireland

(Received December 1999; accepted December 1999)

The conformations of the chains constituting the hydrophilic component of alkyl monolayers and bilayers are investigated by performing molecular dynamics atomistic simulations on these systems at different temperatures. Several monitoring techniques are used to reveal the chain conformations, including atom pair radial distribution functions, evolutions of the torsional angles over thousands of timesteps, frequency distributions of the torsionl angles and 'snapshot' plots of the atomic configurations. These methods consistently testify to the stability of the *trans* (fully extended) character of the strain-free alkyl chains up to room temperature. The chains retain much of this conformation even when the layers are compressed by the application of pressure, to which the chains respond by 'folding' at the ends attaching them to the substrate planes while maintaining directions which are mainly normal to these planes. A non-zero gap between the layers is also maintained. A pressure of about 50 kbar abruptly causes all motion in the chains to cease, resulting in a highly ordered lattice structure.

Keywords: Pressure effects; alkyl chain bilayers; chain conformations; atomistic simulation; molecular dynamics

1. INTRODUCTION

The occurrence of bilayers in nature as micelles and cell membranes and in engineering science as lubricated contacts between plane solids has stimulated interest in the properties and behaviour of these systems. Their response to changes in temperature and pressure, for example, is important in understanding the functioning of living cells under extreme conditions such as those of life forms at high temperatures or at ocean depths.

*Corresponding author. e-mail: tblake@tcd.ie

On the physical side, the use of atomic force microscopy and similar methods to investigate film interfaces on a nanometer scale have led to an interest in the structural changes that occur on an atomic level when forces are applied to films confined between surfaces. This interest is intensified by the current quest for microelectronic and micromechanical components that seeks to emulate bulk devices with ones on a nanometric scale [1, 2]. The dynamical behaviour of several such systems has been investigated [3]. An understanding of nanotribology requires a knowledge of the interaction of the components of a single-asperity-contact molecular interface, particularly when subject to forces applied outside the interface [1].

Materials functioning as lubricants have been shown to undergo reorientations of their constituent fibers and to involve changes in conformation in their alkyl chains [4]. The response of these materials to shearing stresses is often manifested as a series of alternating local crystallisation and melting [5, 6]. On a more fundamental level the frictional component of the motion has been interpreted as a resonant transfer of phonon momentum between the moving components [7]. Effects found to be associated with lubrication on an atomic scale have been interpreted to estimate bulk properties such as Young's moduli, shear strengths and friction coefficients and have promoted discussions on the design of materials associated with wear-free friction and even frictionless motion [8].

We recently conducted a series of calculations on short-chain alkyl bilayers which were subject to external forces by imposing random torsions on the C—C linkages to minimise the energy [6, 9]. The imposition of normal and tangential stresses at various separations of the bilayers was shown to lead to conformational changes on the stress-free all-*trans* chains. This occurred both during the mutual penetration of the layers and also during the 'stick-slip' discontinuities that characterised the sliding of one layer over the other. Since the approach used was essentially a static-lattice one in which profiles of the potential energy variation were monitored, it would seem desirable now to complement this using molecular dynamics (MD) to obtain details of the molecular motions underlying the static-lattice results.

2. THE MODEL

Two monolayer films are sandwiched between a pair of restraining coplanar surfaces which will be referred to as substrates. Each film is a monolayer consisting of parallel *n*-butyl chains $CH_3CH_2CH_2CH_2$— which are firmly

attached at their 'CH_2—' ends to a set of ficticious carbon-like atoms $C^{(0)}$ in the substrate plane. The alkyl chains in one monolayer are normal to the substrate, directed with their CH_3 ends towards the chains in the opposite monolayer, thereby defining a bilayer in a 'Y configuration' as shown in Figure 1(a). Since the present investigation is confined to the mutual interaction of the alkyl chains the atomic nature of the substrate will not be considered explicitly.

Following the model used in our Monte Carlo investigation [6] the anchoring atoms $C^{(0)}$ define lattice points in a two-dimensional hexagonal lattice with a spacing of 4.42 Å. That investigation found that such a parameter minimised the lattice energy, and turned out to be close to measured values of chain separations in LB films. The two substrate lattices are initially positioned in such a way that each alkyl chain in one layer is aligned with an inter-chain channel in the opposite layer as shown in Figure 1(b).

The alkyl chains are placed in a series of different 'contacts' which are defined by a 'separation parameter' z_{tt} which, prior to the relaxation of the chains, measures the tip-to-tip distance along the **z** axis between the hydrogen atoms on atom $C^{(4)}$, *i.e.*, between the methyl extremeties of the chains. If z_{tt} is positive it is equal to the gap between the initially fully-extended chains in the two layers. If negative, the layers are set to penetrate, or interdigitate. In these calculations a lattice is defined by a cell consisting of 18 butyl chains – nine in each of the two monolayers as illustrated in Figure 1(b).

Various structure-determining methods have established that in monolayers and bilayers the alkyl chains are in fully-extended (all-*trans*) conformations. This report describes the application of molecular dynamics at different temperatures to find how this structure is modified when the separation of the layers z_{tt} is changed by the application of pressure resulting in the possible enmeshing of the bilayers. This would occur for example when the monolayers function as lubricants. The conformations of the butyl chains are defined by the sets of dihedral angles φ_1, φ_2, φ_3 and φ_4 which respectively measure the torsions around the three C—C bonds as shown in Figure 1(a). The angles are defined with the sense that 0° corresponds to *trans* and 180° to *cis*.

The calculations in this work were conducted on the model described in which all the atoms were considered explicitly. The molecular dynamics program DL-POLY [10] was used, supplemented by code specifically written to process some of the output data of this program. Since the temperature of the system and the spacing of the substrate planes was subject to controlled restraints, the MD was run at a NVT mode with an Evans

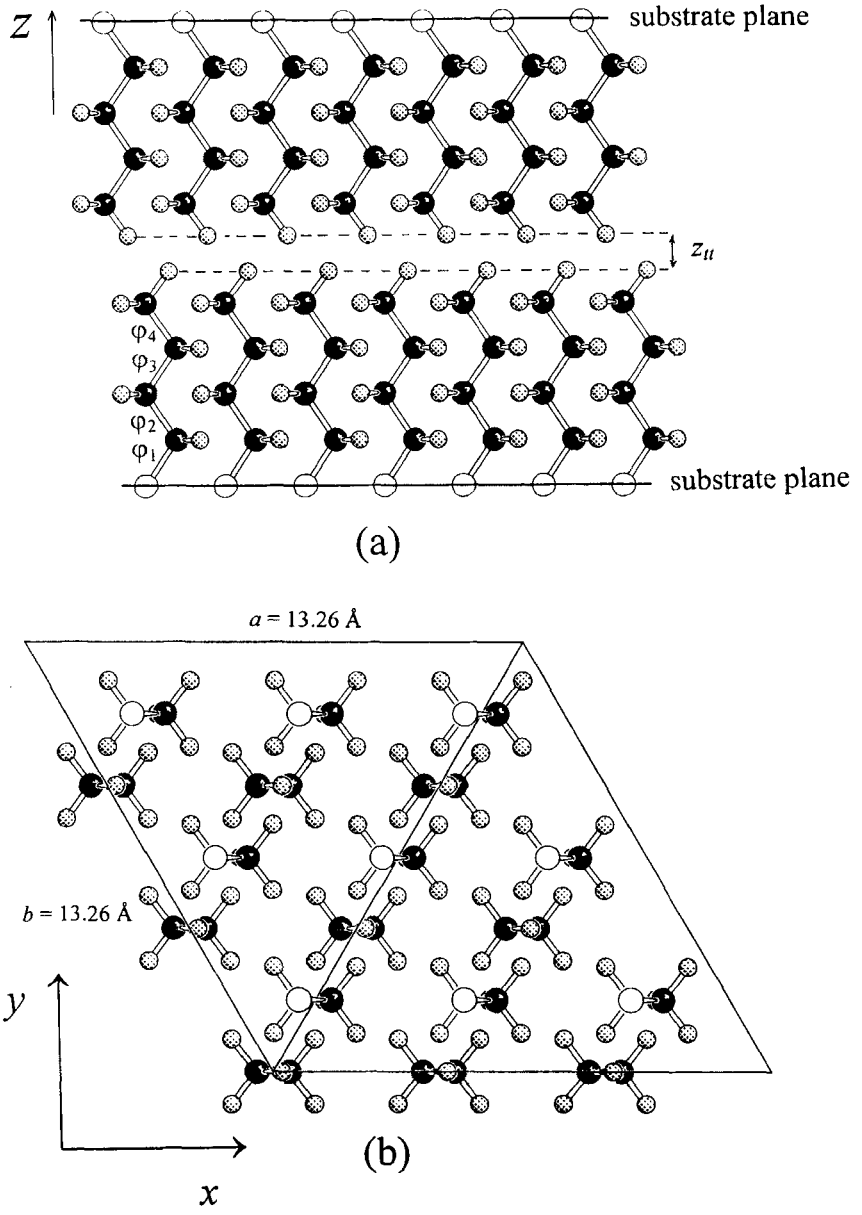

FIGURE 1 Model of the pseudo-hexagonal alkyl bilayer used in this work. The model is viewed (a) along the **a** axis, normal to the chains and (b) along the directions of the (initially all-*trans*) chains. The orthogonal set **x**, **y**, **z** referred to in the text are positioned with **x** and **z** respectively parallel to **a** and **c**. For clarity the structure is drawn with a chain separation d greater than its lowest-energy value.

thermostat with the timestep (ts) set to 0.001 picosecond. The atomistic 'potentials' (energy functions) defining the force field were the Williams IV set for hydrocarbons [11]. These were supplemented by a bond angle distortion potential $V(\theta)=(1/2)k(\theta-\theta_0)^2$ with $k=12.42$ ev rad^{-2} for C—C—C, $k=5.2431$ ev rad^{-2} for H—C—C and $k=3.558$ ev rad $^{-2}$ for H—C—H as used in our previous static lattice calculations on polymers [12]. Bond lengths were constrained to standard values r(C—C) = 1.535 Å, r(C—H) = 1.10 Å and no bond torsional functions were used.

3. MONOLAYERS

3.1. Radial Distribution Functions

The (C, C), (C, H) and (H, H) radial distribution functions $g_{CC}(x)$, $g_{CH}(x)$ and $g_{HH}(x)$ monitor the number of atom pairs found over a range of interatomic distances at the temperatures selected for the molecular dynamics, at 10, 100, 200 and 300 K. The (C, C) distribution functions (rdf) traces in Figure 2(a) show a peak at $r=3.9$ Å which is close to the 3.917 Å distance of the 1, 4 carbon–carbon *trans* linkage [$C^{(1)}$, $C^{(4)}$] at 3.9 Å. The distance between C atoms 1 and 4 would decrease to 3.05 Å for a *gauche* linkage and to 2.69 Å for *cis*. Even a torsion as small as 30° would reduce the distance to 3.85 Å, where the values of $g(r)$ at the highest temperatures are only half those at the maxima. The fact that the peak is not significantly blunted over the substantial temperature range considered, and that it is maintained at $r=3.90$ Å, shows the inherent persistence of *trans*-like linkages in this system of alkyl chains.

The (C, C) peak at $r=4.40$ Å, which is very prominent at 10 K, corresponds to the translational distance of the chains along the crystalline **a** and **b** axes, and therefore constitutes a very common inter-chain distance in the regular, static lattice. As an inter-chain vector, however, it is sensitive to the relative positions of the chains, and does indeed decrease quite rapidly with increasing temperature. The position of the (C, C) peak at 5.09 Å shows that it contains a contribution from the 5.096 Å distance $C^{(0)}C^{(4)}$ between the terminal methyl carbon and the substrate plane carbon of the all-*trans* chain, but as there is only one such atom pair separation per chain, its amplitude is too large to be solely due to this. The distance is also close to the 5.101 Å separation between any C atom in one chain and the third C atom in its coplanar nearest-neighbour chain. Using primes to denote atoms on neighbouring chains, as there are seven such 'knight's move' displacements $C^{(i)}C^{(i+2)'}$ to only one end-to-end

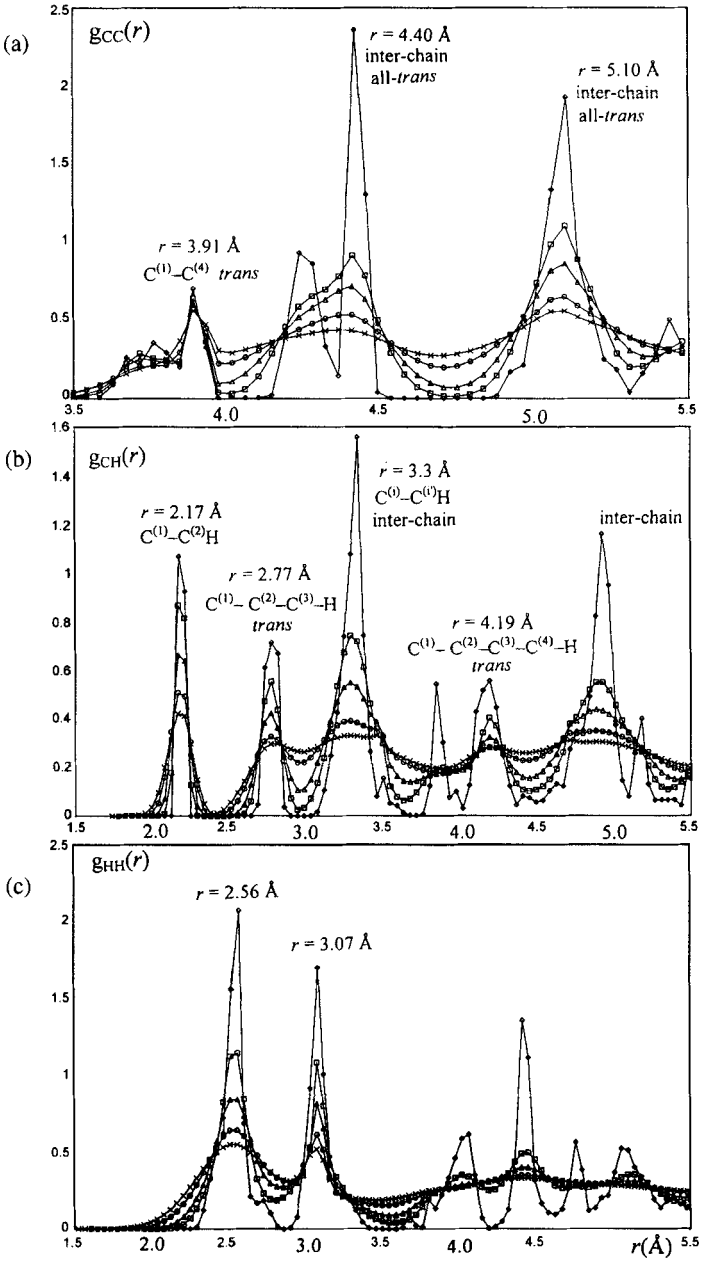

FIGURE 2 (C, C), (C, H) and (H, H) radial distribution functions in the monolayer at different temperatures: 10 K(– ◇ –), 50 K(– □ –), 100(– Δ –), 200 K(– ○ –) and 300 K(– × –).

displacement $C^{(0)}C^{(4)}$, the former would dominate the peak. An *inter*chain separation such as that of the 4.40 Å peak succumbs more readily to small conformational changes than *intra*chain distances, as shown by its fast decay with increasing temperature. Unlike the 4.40 Å peak, however, the $C^{(1)}C^{(3)'} + C^{(0)}C^{(4)}$ maximum remains at 5.09 Å even to room temperature. This may be due to the persistent *trans* linkages in the butyl chain.

The (C, H) peak at $r = 2.17$ Å in Figure 2(b) is for $C^{(1)}—C^{(2)}H$ whose separation is not affected by bond torsion, and so persists to high temperature. The maximum at 2.77 Å shows that the intra-chain ($C^{(1)}$, $H^{(6)}$) distance in the fragment $C^{(1)}—C^{(2)}—C^{(3)}H$ (which is 2.77 Å when $C^{(2)}—C^{(3)}$ is a *trans* link in the 4-C atom chain containing it) is preserved to high temperatures. The peak is broadened by the increased torsional motion, and is affected by the broadening of the ($C^{(1)}$, $H^{(3)'}$) contribution from the inter-chain fragment $C^{(1)}, C^{(2)'}H^{(3)'}$. We believe that the high-temperature survival of the 4.19 Å maximum can also be ascribed to the 4.20 Å *trans* intra-chain distance between the first and last written atom in the chain $CH_2—CH_2—CH_2—CH_2$, although there is also an inter-chain contribution to the peak, blunting (but not eliminating) it at higher temperatures. The prominent rdf at $r = 3.3$ Å is a short inter-chain separation $C^{(i)}—C^{(i)'}H$, and that at about $r = 4.9$ Å is a superposition of several inter-chain distances.

The (H, H) distances are very sensitive to chain conformation, and in fact the (H, H) rdf traces in Figure 2(c) have only two maxima (at 2.56 Å and 3.07 Å) which persist to room temperature. These two are close to *four* different intrachain (H, H) separations in the all-*trans* chain which happen to fall into *two* narrow ranges. In the chain $H^{(1)}H^{(2)}C^{(3)}—C^{(4)}H^{(5)}$ $H^{(6)}—C^{(7)}H^{(8)}H^{(9)}—C^{(10)}$ the first of these are the $H^{(1)}H^{(5)}$ and $H^{(1)}H^{(8)}$ separations, at 2.52 and 2.55 Å respectively, the second $H^{(1)}H^{(6)}$ and $H^{(1)}H^{(9)}$ which are at 3.07 and 3.09 Å. The remaining peaks, which are interchain, are mainly washed out by the thermal broadening.

In summary, the rdf traces show that despite thermal activity the alkyl chains retain much of their *trans* conformation from very low temperatures to 300 K, but that the relative motions of the chains frequently obscures the rdf peaks appropriate to *inter-chain* atom pairs at higher temperatures.

3.2. Conformational Evolution

Figure 3 shows the changes in the conformational structure of *one* of the 18 alkyl chains in the bilayer simulation cell over a picosecond interval (1000 timesteps) after the establishment of thermal equilibrium at

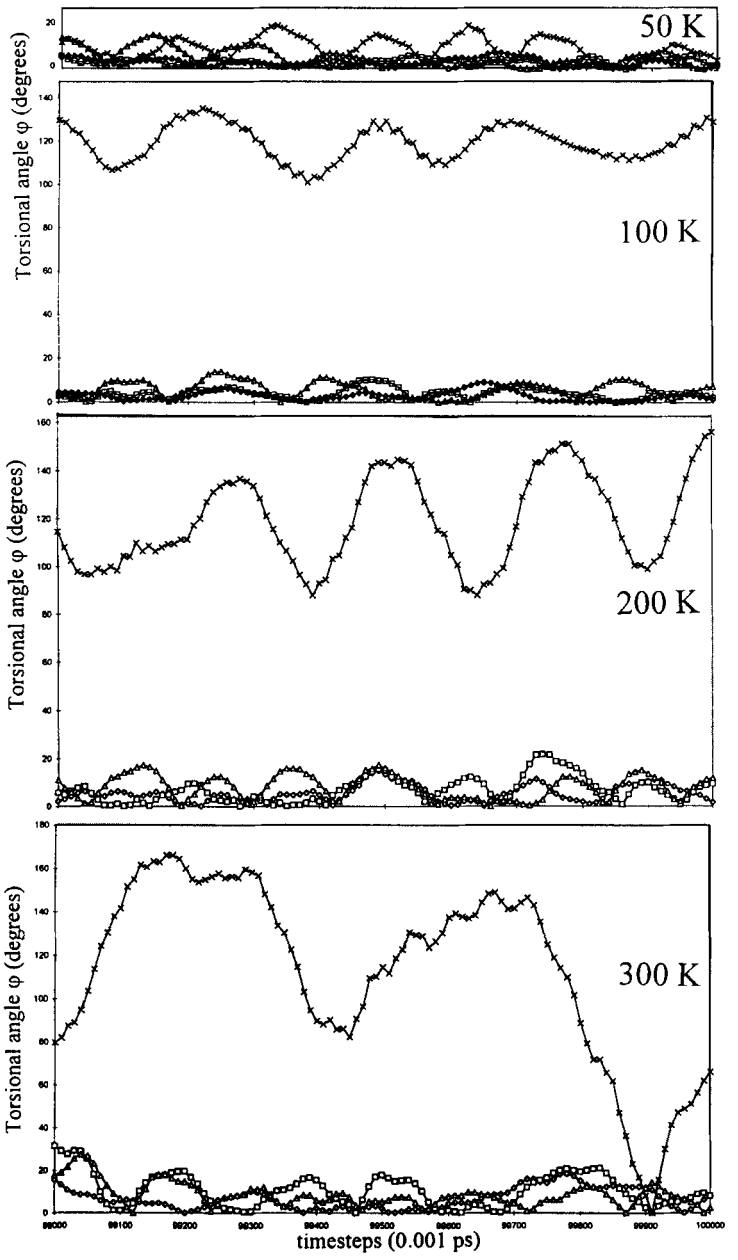

FIGURE 3 Conformational evolution of the four C—C linkages in one of the butyl chains in the monolayer at various temperatures over a period of 1000 timesteps (1 ps) after the establishment of thermal equilibrium. The same vertical scale is used for all the plots, and the symbols are: –◇–(link 1), –□–(link 2), –Δ–(link 3) and –×– (link 4, *i.e.*, methyl).

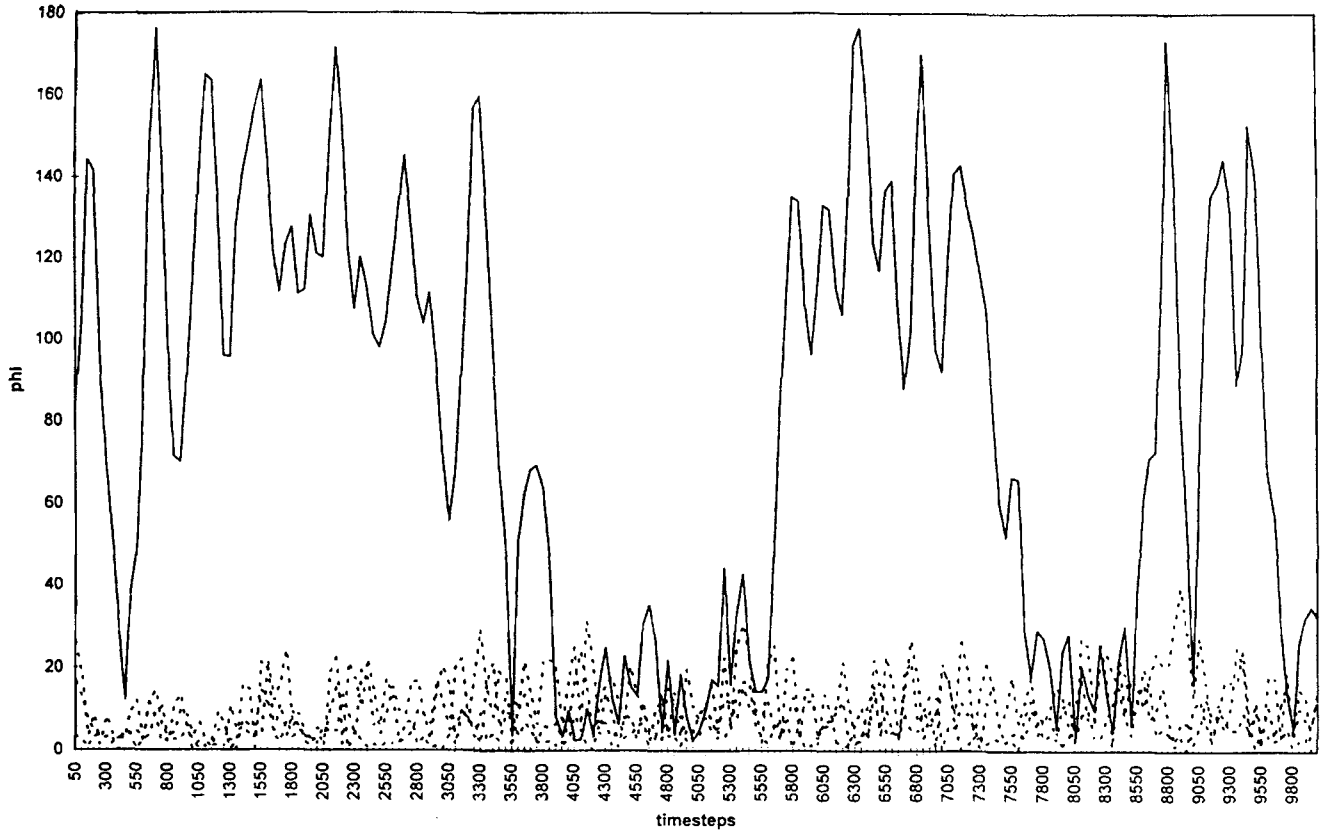

FIGURE 4 Conformational evolution of the butyl chain over 10 000 timesteps (10 ps) in the monolayer at 300 K. The continuous trace monitors the CH_3 reorientation (link 4) while the dotted lines describes the other three links. Note the frequent jumps of the methyl between equivalent positions centered at 0° and 120°.

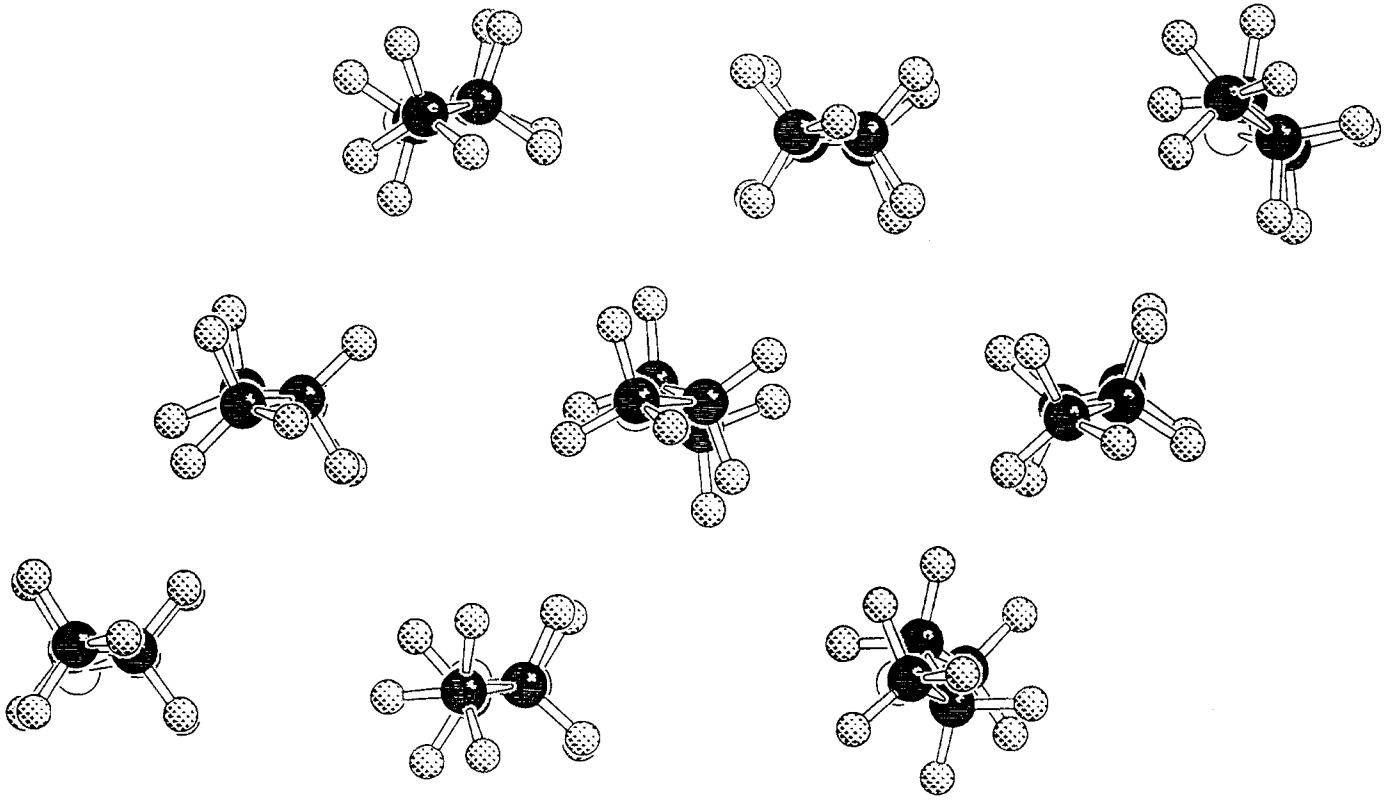

FIGURE 5 A 'snapshot' atomic plot showing the conformations of the monolayer butyl chains at 300 K after the establishment of thermal equilibrium. The essentially *trans* conformations of the chains is evident.

temperatures of 50, 100, 200 and 300 K. In fact, the features of the other 17 butyl chains in the cell exhibit such broadly similar features that choosing any of them would lead to the same conclusions as the one arbitrarily selected for discussion in this section.

At the lower end of the temperature range changes in the four torsional angles are small and correspond to librations, or restricted internal rotations around the C—C bonds with rather uniform frequencies. The figures give only positive values of the torsional angles, but the frequent cusps of the curves at zero torsional angle shows that the librations of the chains are centered around their all-*trans* conformations even at room temperature. The greater amplitude of the φ_4 fluctuation indicates the expected greater reorientational freedom of the terminal methyl group. The 100 K trace shows a transition from a libration in which the φ_4 fluctuations are centered at 0° to those in which they are centered at the sterically equivalent 120° conformation.

In Figure 4, where the (φ_4 trace is taken over *subsequent* 1000 timesteps, repeated occurences of 120° conformational jumps at room temperature are evident as the angles, on which the librational signals are centered, switch between $\varphi = 0°$ and $\varphi = 120°$. Following 'quiescent' periods, when the librational amplitude of the methyl is similar to those of the other butyl links, the amplitudes may increase markedly as the methyl group undergoes complete (360°) rotations.

3.3. Conformational Structure

Figure 5 shows a typical 'snapshot' atom plot of the bilayer at an arbitrary timestep after equilibration at the higher end of the temperature range, 300 K. A comparison of the figure with Figure 1 shows that although some torsions have occurred around the C—C bonds in two of the nine chains visible in the plot, the remainder have retained much of their original conformation. This supports the picture presented by the radial distribution functions and the torsional history plots of the inherent resilience of the *trans* linkage. This conformational feature may therefore be usefully applied to describe most of the nine chains in the 'snapshot' figure.

4. BILAYERS

The application of pressure between film-coated surfaces was simulated by bringing the constituent layers of a Y-configuration bilayer system to a

configuration in which mutual penetration the alkyl chains would occur if they remained 'fully extended'. The MD simulation was then run at constant volume and constant temperature (Evans NVT mode) with the object of examining the result on chain conformation.

Starting from the bilayer configuration described in Section 2, with a chain-end tip-to-tip distance z_{tt} of $+2.0$ Å, rdfs and chain torsions were calculated at decreasing values of z_{tt}. This parameter was defined as the distance between the ends of the alkyl chains in their *initial* configurations in the two layers, so that negative values implied interdigitation (penetration) of the layers. However it must be recalled that at this point all the alkyl chains were in all-*trans* conformations and therefore 'fully extended'. Any conformational change in the chains would of course increase the gap between their tips in the **z** direction; as a result negative z_{tt} need not necessarily imply that the layers still penetrate. This question will have to be determined by an examination of the atomic coordinates of the relaxed chains.

4.1. Pressure and Internal Energy Changes

Figure 6 shows how the pressure components along the **x**, **y** and **z** axes in the bilayer lattice respond to the compression, varied *via* the separation parameter z_{tt}. (See Fig. 1 for the identification of the directions.) The nature of the lattice structure requires these components not to be equal, and the pressure anisotropy is maintained over the compression range considered, with the z-component remaining the smallest. This may be explained by noting that a chain sequence of *trans* linkages in the xz plane, directed along **z**, is on the whole less compliant to a force along **x** than along the other two directions, since in these the steric pressure may be relieved possibly by interdigitation or by folding of the chains. The manner in which the chains in fact respond to the pressure will be seen below.

Figure 6 shows that the *normal* pressure (*i.e.*, along **z**) changes very gradually as the parameter z_{tt} characterising the bilayer separation decreases from $+0.5$ to -1.5 Å. Its value remains at just under 20 kbar, agreeing with the 18 kbar value derived for the same range from our Monte Carlo treatment of the same system [6]. Over the subsequent compression of the bilayer through 1.0 Å the normal pressure increases rapidly to 40 kbar. At $z_{tt}=2.9$ Å the pressure abruptly passes through a strong minimum in the **x** direction and weaker minima in the other two directions before resuming its rise with increasing compression. This behaviour shows that there is a sudden, partial relief from congestion particularly in the **x** direction, suggesting a structural change.

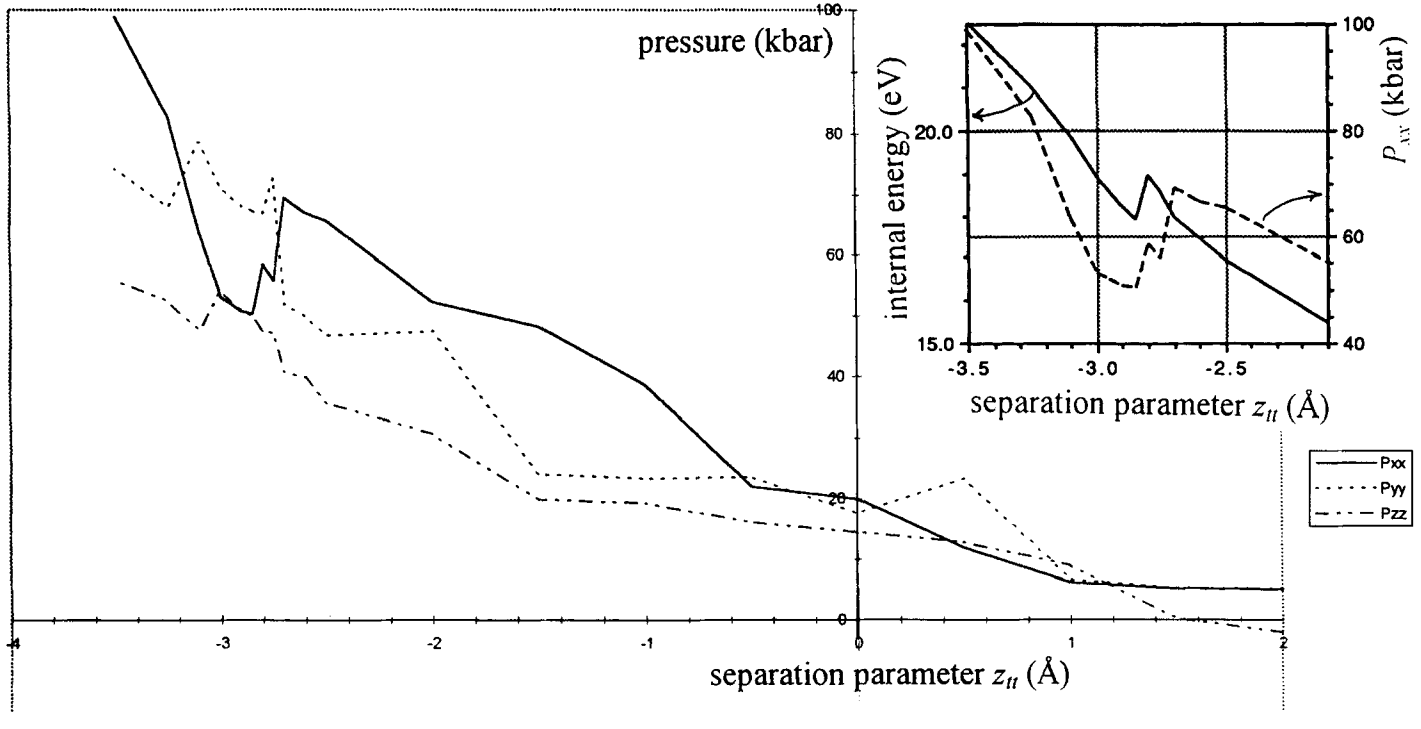

FIGURE 6 Components of the pressure tensor of the bilayer at 100 K as a function of z_{tt}. The inset is a double-ordinate plot correlating the internal energy of the bilayer and the x-component of the pressure with changing z_{tt}. It shows the effect of the structural phase change in the region around $z_{tt}=2.9$ Å.

The inset to Figure 6 shows that the internal energy increases with compression, but at the same point as that associated with the pressure changes ($z_{tt} = 2.9$ Å) it also shows a discontinuous shift to lower energy, suggesting a structural change at this condition. The behaviour of the bilayer at this compression will be discussed below.

4.2. C, C Radial Distribution Functions

In this section we concentrate on the (C, C) rdfs which are more useful than those of (C, H) and (H, H) to describe chain conformations. The $g_{CC}(r)$ curves in Figure 7 show the result of reducing the bilayer separation parameter z_{tt} at 100 K. As high-temperature motions sometimes mask features of the dynamics of the atoms and groups, in the following discussion we shall mainly confine our attention to the lower end of the stated temperature range, *i.e.*, the results at $T = 100$ K.

Of the three principal peaks discussed in Section 2 (those at r values of 3.9, 4.4 and 5.09 Å) the 3.9 Å peak is the most persistent, remaining sharp down to the smallest z_{tt} value considered. This again indicates the strength of the trans $C^{(1)}C^{(4)}$ linkage even in the presence of steric congestion. Interestingly, the three peaks initially sharpen as the layers approach from $z_{tt} = +2.0$ to $+1.0$ Å, suggesting a stabilising interaction of the layers as the bilayer is formed.

As z_{tt} decreases to values corresponding to a pressurised bilayer most of the peaks broaden and decay, but some new, prominent ones appear whose amplitudes and positions change rapidly with decreasing z_{tt} in the region below $r = 3.3$ Å. Then at $z_{tt} = -3.0$ Å, where the normal pressure is 50 kbar, the maxima at 2.90 and 2.99 Å correspond to an intrachain $C^{(1)}$—$C^{(4)}$ distance in $C^{(0)}$—$C^{(1)}$—$C^{(2)}$—$C^{(3)}$ in which a torsion close to 120° from *trans* has occurred around $C^{(1)}$—$C^{(2)}$ (r would be 2.94 Å for pure *gauche*). This interpretation is confirmed by the molecular plot of the chains in Figure 8 which shows their configuration when $z_{tt} = -3.0$ Å. It is clear from the diagram that unlike the conformations at other z_{tt} values the chains in the cell now have a remarkably high degree of order. Concerted with the change to this ordered state a *gauche* transition has occurred in *all* the alkyl chains in the cell. Although the carbon skeleton $C^{(1)}$—$C^{(2)}$—$C^{(3)}$—$C^{(4)}$ of the butyl chains still retains its largely *trans* conformation as noted above, and most of the chain is still aligned normal to its substrate plane, the folding of the chains towards the substrate planes as a result of the *gauche* transition effectively shortens the remaining length of the chains which is directed normal to the substrate.

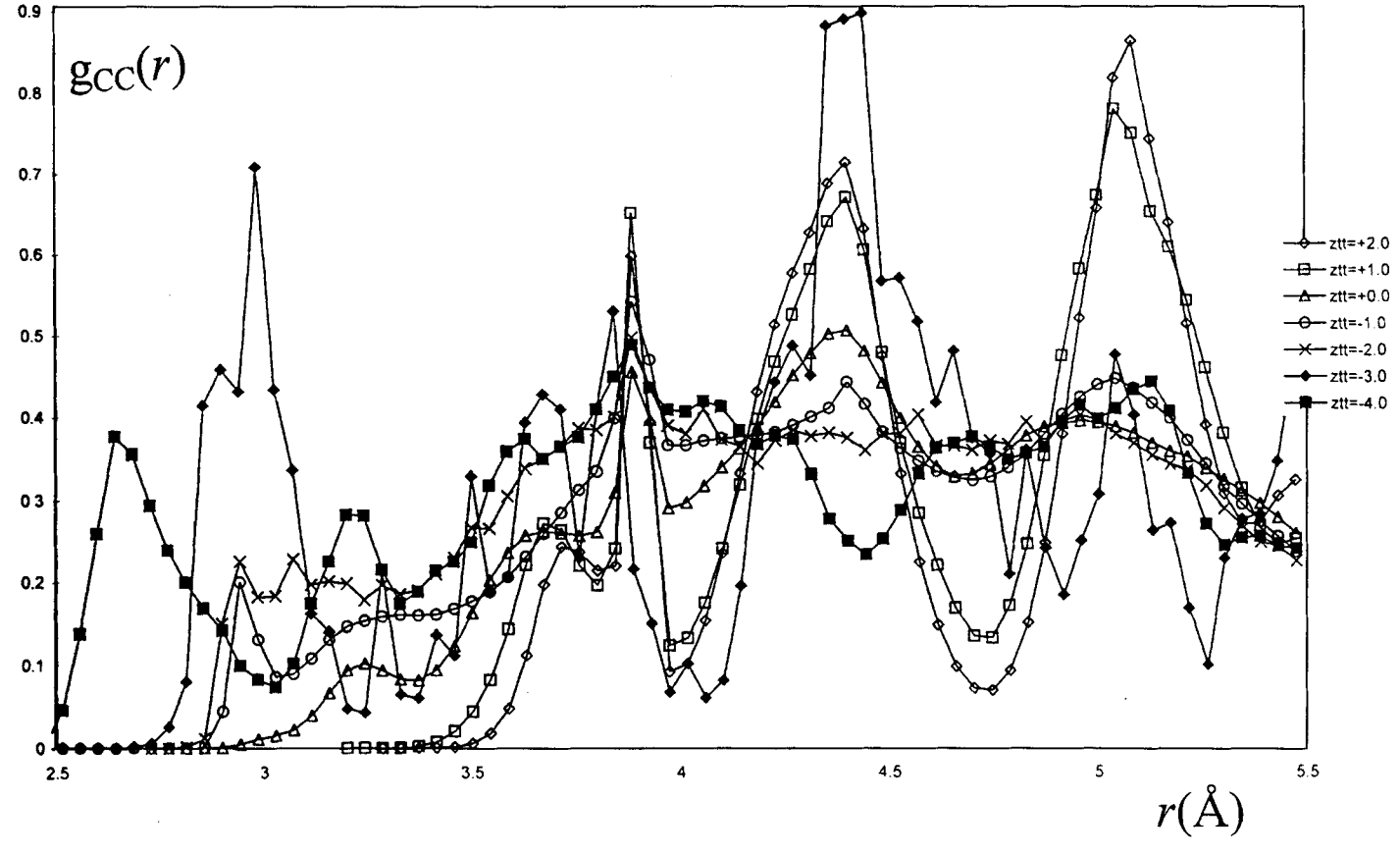

FIGURE 7 The (C, C) pair radial distribution functions of a butyl bilayer at different values of the bilayer separation parameter z_{tt} (see text).

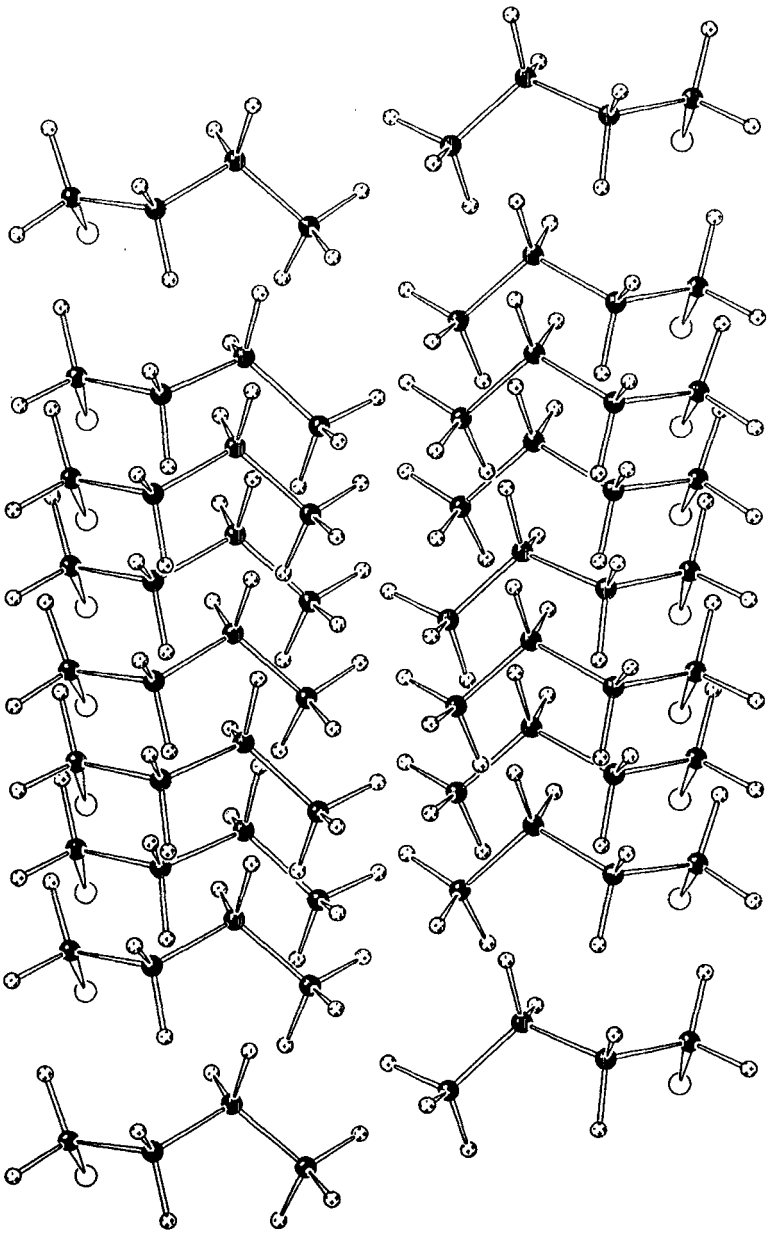

FIGURE 8 A 'snapshot' atomic plot of the bilayer at high compression ($z_{tt} = -3.0$ Å). The chains, which are strongly tilted on the substrate planes, show a high degree of order and are still aligned largely normal to the substrates. The gap between the layers is maintained at all stages of the compression of the layers.

This 'shortening' of the chains eliminates the initial 3.0 Å penetration (implied by $z_{tt} = -3.0$ Å) so that on relaxation the chains show a reluctance to interdigitate and modify their conformation so as to *retain the gap* between the monolayers.

On reducing z_{tt} further from -3.0 to -4.0 Å the rdf showing the *gauche* linkage in $C^{(1)}—C^{(2)}—C^{(3)}—C^{(4)}$ at $r \approx 2.94$ Å shifts to 2.65, which is close to the 2.69 Å corresponding to *cis*. Again the molecular plots show that the butyl skeletons are normal, but now each $C^{(0)}—C^{(1)}$ bond pushes the $C^{(1)}$ atom *into* the plane of the substrate $C^{(0)}$ atoms. This indicates that the validity of the model has broken down by the time z_{tt} reaches -4.0 Å., since it does not include the atoms of the substrate material. We therefore impose a lower range limit on z_{tt} at -3.5 Å.

The folding of the chains near their points of attachment to the substrate and the accompanying sharpening of the rdf peaks show that the layers undergo a sharp structural change involving increased order when the normal pressure in the bilayer approaches the critical value of 50 kbar.

4.3. Conformational Evolution

It would be expected that the structural discontinuity at $z_{tt} = -3.0$ Å should be revealed also in the motions occurring in the alkyl chains. Figure 9 shows the conformational evolution of the terminal methyl groups on the 18 chains in the simulation box at separation parameters $z_{tt} = +2.0$, $+1.0, 0.0, -1.0, -2.0, -3.0$ Å over a period of 1000 timesteps (*i.e.*, 1 ps) after the establishment of equilibrium. We restrict the display to the CH_3 groups as they show more activity and features of interest than the other torsional links in the chain.

The torsions show that for moderate values of the separation parameter z_{tt} the CH_3 librations remain centered at their 0° or 120° conformations, so that under these conditions the threefold axial symmetry of the CH_3 sites on different chains appears to be retained. (Because the φ range in the figure is 0° to 180°, an angle $\varphi = 240°$ appears as 120° and negative φ values are reflected up into the positive range.) As z_{tt} decreases to -1.0 Å the curves show an increasing librational amplitude and the methyls begin to undergo 120° jumps. At $z_{tt} = -2.0$ Å the amplitude decreases as a result of the confinement imposed on the chains, which also results in the inequivalence of the sites for CH_3 groups on different chains. Finally, at $z_{tt} = -3.0$ Å the methyls' libration amplitudes decrease dramatically, showing that they become securely fixed in one of their three almost equivalent orientations. This abrupt change is consistent with the sudden sharpening

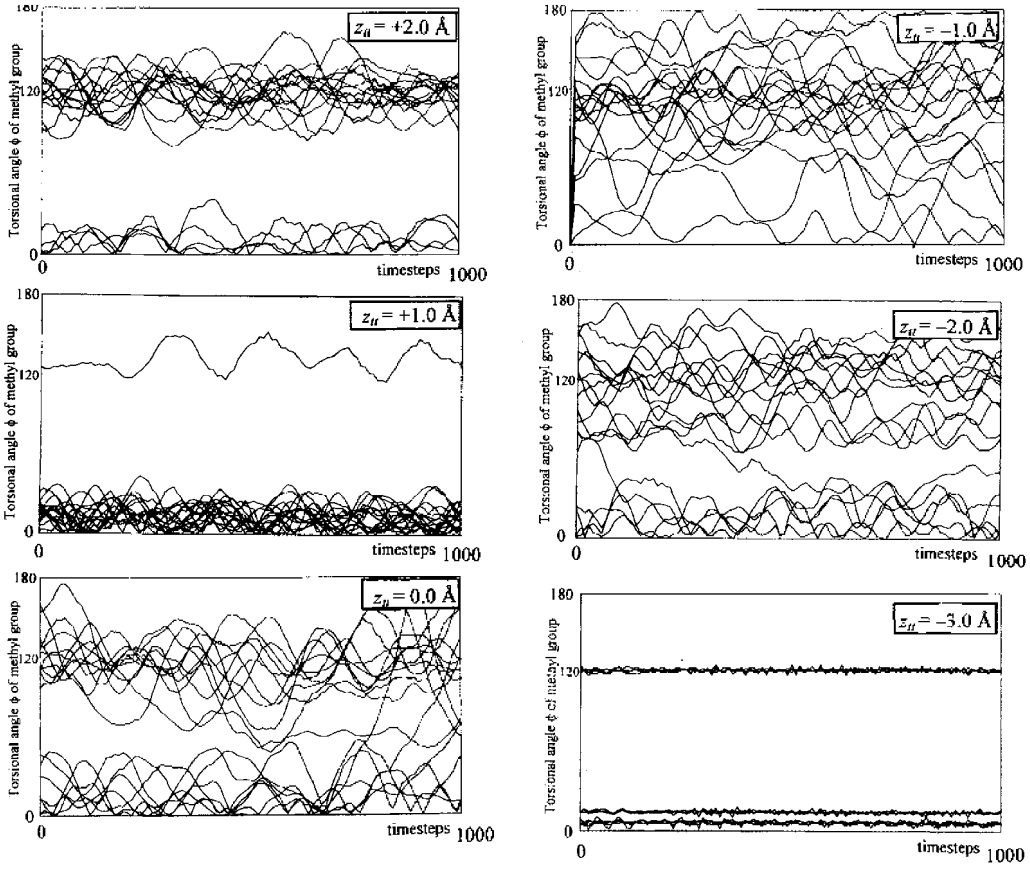

FIGURE 9 The conformational evolution of the CH_3 groups on all 18 butyl chains in the bilayer at various compressions (values of the bilayer separation parameter z_{tl}) over 1000 timesteps (1 picosecond) after the establishment of thermal equilibrium.

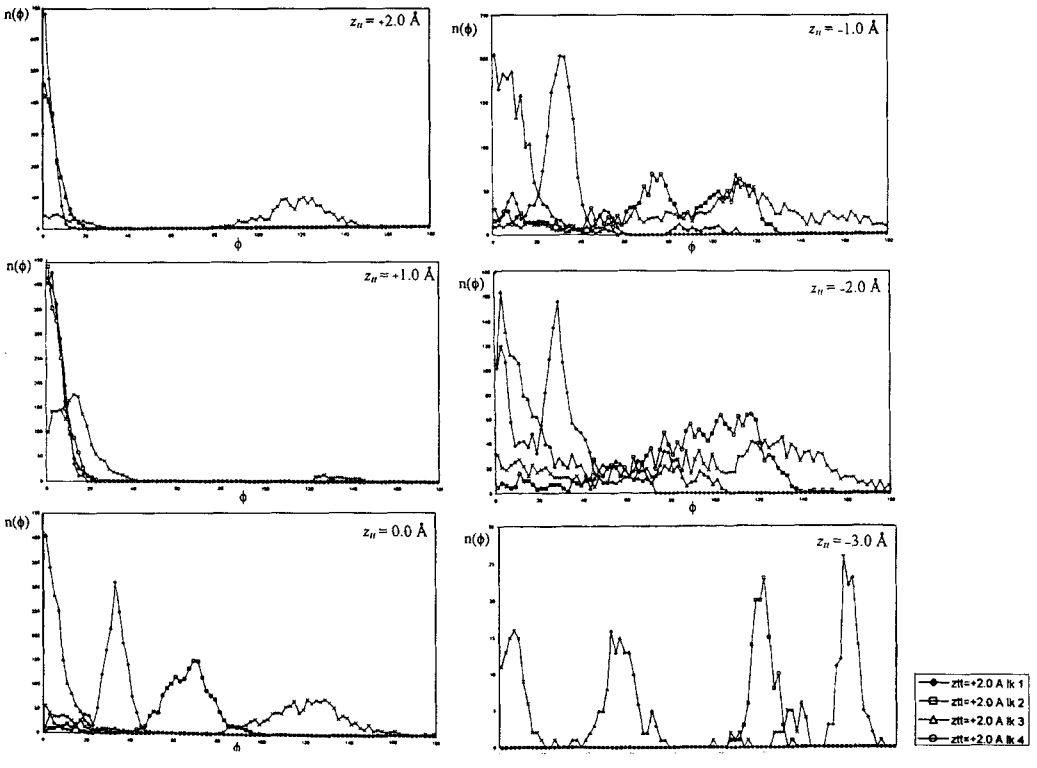

FIGURE 10 Torsional distribution curves of the four butyl C—C links φ_1, φ_2, φ_3, φ_4 taken from all the chains in the simulation for 1000 timesteps (1 picosecond) after thermal equilibrium. The compression changes the conformations from all-*trans* at $z_{tt} = +2.0$ Å through regions of reduced order at greater compressions, to a highly ordered structure at $z_{tt} = -3.0$ Å.

of the rdf peaks (Fig. 7) at the same z_{tt} value and with the conformational order depicted by the atomic positions in Figure 8.

4.4. Distribution of Torsional Angles

Another structural parameter often employed to describe chain conformations is the frequency of occurrence of torsional angles in the chains. Figure 10 shows torsion distribution curves in the range $0° \leq \varphi \leq 180°$ for periods of 1 picosecond after equilibrium, at the same conditions as those of the conformational evolution curves in Figure 6. Four curves are displayed for each of the six z_{tt} values defined in the last two subsections – one for each of the four C—C links in the butyl chain.

Except for φ_4, which describes the torsion of the terminal methyl groups, and which are distributed about 20° on either side of the equivalent $\varphi = 0°$ and $\varphi = 120°$ positions, the angular distribution peaks are prominent at $\varphi = 0°$ for positive z_{tt}. As the layers are compressed to z_{tt} values 0.0, −1.0 and −2.0 Å, the peak for φ_1 (though still sharp) is displaced to 30–35°, φ_2 spreads over a large range of angles, but φ_3 retains its maximum value at $\varphi = 0°$. This behaviour is consistent with the conformations deduced above from the radial distribution functions of Figure 7, the persistance of the *trans* linkage of the butyl carbon skeleton is shown by the 0° peak of φ_3, and the shift of φ_1 to 30° implies a *tilt* of the chains, commonly observed in fully-extended alkyl-chain monolayers. At $z_{tt} = -3.0$ Å the torsion distribution curve changes as markedly and as abruptly as did the radial distribution and the conformational evolution curves. With the onset of crystallisation at 50 kbar normal pressure the torsion φ_1 of the $C^{(0)}$—$C^{(1)}$ bond jumps from 30° to 160° indicating a tilt of the bond almost into the substrate plane. The $C^{(1)}$—$C^{(2)}$ is closely *gauche*, with a sharp peak at $\varphi_2 = 120°$, while the third link $C^{(2)}$—$C^{(3)}$ measured by φ_3 that was previously 0°, and made the butyl chain *trans*, is now 50–60°; conferring non-planarity on the carbon skeleton of the alkyl chain of the crystallised bilayer.

5. CONCLUSIONS

The chain conformations in alkyl films have been monitored by pressure components, internal energy changes, atom-pair radial distribution functions, conformational evolution and torsional distribution curves as well as 'snapshot' atomic coordinate plots under various stress conditions.

The results testify to the stability of the *trans* conformations of the alkyl chains in the monolayer and in the bilayer under liquid-like conditions in which the chain has substantial librational freedom. At temperatures up to 300 K, despite a torsion around the $C^{(1)}$—$C^{(2)}$ bond and a tilting of the chain (torsion around $C^{(0)}$—$C^{(1)}$) the *trans* linkages in the 4-atom *carbon skeleton* of the butyl chain largely survive the imposition of pressure and even retaining their general direction normal to the substrate plane. The tilting of the chains at their points of attachment to the substrate precludes the mutual penetration of the alkyl layers by interdigitation, and results in the survival of the inter-layer gap.

With increasing pressure, the monitoring methods show that the chains undergo an abrupt change of conformation to one in which the butyl carbons are no longer planar as the atoms become locked into an ordered, close-packed structure with greatly reduced librational freedom. The 'crystallisation' of the previously liquid-like, highly flexible alkyl chains should result in a considerable change in the phonon band structure associated with the systems in relative motion. Since friction on an atomic level has been interpreted as a resonant transfer of phonon energy between the moving surfaces [7], the motion would be expected to be substantially affected by the pressure-induced change.

Friction effects are currently being performed by studying chain conformational changes and relaxations when one of the layers is displaced in the *xy* plane (as was previously done on a Monte Carlo level [6, 9]). This work will be described in a subsequent paper.

References

[1] Krim, J. (1997). "Friction at the atomic scale", *Lubrication Engineering*, **53**(1), 8.

[2] Maboudian, R. (1998). "Adhesion and friction issues associated with reliable operation of MEMS", *MRS Bulletin*, **23**(6), 47; Maboudian, R. (1998). "Surface processes in MEMS technology", *Surface Science Reports*, **30**(6), 209; Seife, C. and Crystall, B., "There's the rub", *New Scientist*, 17 October, 1998, p. 30.

[3] Chugg, K. J. and Chaudhri, M. M. (1993). "Boundary lubrication and shear properties of thin solid films of dioctadecyl dimethyl ammonium chloride (TA100)", *J. Phys. D: Appl. Phys.*, **26**, 1993; Mate, C. M., McClelland, G. M., Erlandson, R. and Chiang, S. (1987). "Atomic scale friction of a tungsten tip on a graphite surface", *Phys. Rev. Lett.*, **59**, 1942.

[4] Adolf, D. B., Tildesley, D. J., Pinches, M. R. S., Kingdon, J. B., Madden, T. and Clark, A. (1995). "Molecular dynamics simulations of dioctadecyl-dimethylammonium chloride monolayers", *Langmuir*, **11**, 237; Vacatello, M., Yoon, D. Y. and Laskowski, B. C. (1990). "Molecular arrangements and conformations of liquid *n*-tridecane chains confined between two hard walls", *J. Chem. Phys.*, **93** 779; Zhang, H., Kulshrestha, N. P., Woehler, S. E. and Wittebort, R. J. (1996). "Alkyl chain dynamics in perovskite bilayers and their variation with structural phase as studied by powder and single crystal NMR", *J. Chem. Phys.*, **105**, 2891; Briscoe, B. J., Stuart, B. H. and Thomas, P. S. (1993). "Solvent induced morphological changes to polycarbonate", *Proceedings of MRS WearMeeting*;

Briscoe, B. J. and Thomas, P. S. (1994). "Structure-property relationships in thin solid poly (methylmethacrylate) boundary films", *Proceedings of the 20th Leeds-Lyon Symposium.*

[5] Schoen, M., Diestler, D. J. and Cushman, J. (1993). "Shear melting of confined solid monolayer films", *Phys. Rev. B*, **47**, 5603; Gee, M. I., McGuiggan, P. M., Israelachvili, J. N. and Homola, A. M. (1990). "Liquid to solidlike transitions of molecularly thin films under shear", *J. Chem. Phys.*, **93**, 1895; Yoshizawa, H., Chen, Y.-L. and Israelachvili, J. N. (1993). "Recent advances in molecular level understanding of adhesion, friction and lubrication", *Wear*, **168**, 161; Yoshizawa, H. and Israelachvili, J. N. (1993). "Fundamental mechanisms of interfacial friction. 2. Stick-slip friction of spherical and chain molecules", *J. Phys. Chem.*, **97** 11300; Gao, J., Luedtke, W. D. and Landman, U. (1997). "Structure and solvation forces in confined films: Linear and branched alkanes", *J. Chem. Phys.*, **106**, 4309.

[6] Corish, J. and Morton-Blake, D. A. (1998). "Atomic-scale simulation of lubricated motion", *Molecular Simulation*, **21**, 41.

[7] Glosli, J. N. and McClelland, G. M. (1993). "Molecular dynamics study of sliding friction of ordered organic monolayers", *Phys. Rev. Lett.*, **70**, 1960.

[8] Krim, J. (1998). Fundamentals of friction", *MRS Bulletin*, **23**(6), 20; Krim, J., "Friction at the atomic scale", *Scientific American*, October, 1996, p. 48; Bhushan, B., Israelachvili, J. N. and Landman, U. (1995). "Nanotribology, friction, wear and lubrication at the atomic scale, *Nature*, **374**, 607; Robbins, M. O. and Krim, J. (1998). "Energy dissipation in interfacial friction", *MRS Bulletin*, **23**(6), 23.

[9] Corish, J. and Morton-Blake, D. A., "Atomistic simulations of lubricated motion", *Proceedings of the 19th Risø International Symposium on Materials Science: Modelling of Structure from Microscale to Product*, Ed. Carstensen, J. V., Leffers, T., Lorentzen, T., Pedersen, O. B., Sørensen, B. F. and Winther, G., Risø National Laboratory, Roskilde, Denmark, 1998.

[10] Smith, W. and Forester, T. R. (1996). DL_POLY_2.0: "A general-purpose parallel molecular dynamics simulation package" *J. Molec. Graphics*, **14**, 136.

[11] Williams, D. E. (1967). "Nonbonded potential parameters derived from crystalline hydrocarbons", *J. Chem. Phys.*, **47**, 4680.

[12] Corish, J., Morton-Blake, D. A., Bénière, F. and Lantoine, M. (1996). "Interaction of side-chains in poly(3-alkylthiophene) lattices", *J. Chem. Soc., Faraday Trans.*, **92**, 671.